Physics Letters A 477 (2023) 128896

Contents lists available at ScienceDirect

Physics Letters A

journal homepage: www.elsevier.com/locate/pla

Singularity induced bifurcations in multiple transonic crossings of unsteady self-similar gravitational flows

Wieslaw Marszalek [a], Tewodros Amdeberhan [b,*]

[a] Opole University of Technology, Department of Computer Science, 45-758 Opole, Poland
[b] Tulane University, Department of Mathematics, New Orleans, LA 70118, USA

ARTICLE INFO

Article history:
Received 4 April 2023
Accepted 5 May 2023
Available online 11 May 2023
Communicated by A. Das

Keywords:
Transonic flows
Unsteady gravitational fields
Self-similar solutions
Singular (implicit) ODEs
Singularity induced bifurcations
Matrix pencils

ABSTRACT

A singularity induced bifurcation (SIB) phenomenon is used in this paper to analyze transonic flow in an unsteady gravitational field. Multiple sonic crossings by a single trajectory in the gravitational field are characterized by the divergence of eigenvalues of the linearized model, folded saddles and nodes, as well as the existence of impasse points at the sonic manifold. The analysis is done in the framework of self-similarity shockless solutions. Two particular implicit ODE models of the transonic flows in the gravitational field around a central point mass are analyzed.

1. Introduction

From the vapor cone forming around airplanes flying at around the speed of sound [14], through geologic environments including the CO_2 sequestration [1], geothermal energy development, geysers, and volcano eruptions [12,20], design of viscous flow nozzles [2,5,11], projectile and airfoil flights [7,8,23,24], to traveling wave [3,17] and self-similar numerical solutions in MHD and unsteady gravitational fields [6,15,19], the transonic phenomena and their mathematical analysis attracted a wide interest in the last three decades. In particular, [2] reports that shockless transitions from supersonic to subsonic flow are indeed possible both numerically and theoretically. While single *supersonic-to-subsonic* or *subsonic-to-supersonic* transitions (crossings) are quite well recorded in many engineering and science areas, the cases of multiple such transitions in the same system or experiment (or a mathematical model) are rather scarce, particularly in the context of *smooth* transitions. Two fundamental questions arise:

- Can such *smooth* transonic flows (being solutions of differential equation models) happen two or more times in the case of one trajectory?
- What mathematical tools describe properties of such multiple crossings?

This paper illustrates the fact that the *transonic* solutions in general, and multiple ones in particular, can be characterized in terms of the *singularity induced bifurcation* (SIB) of differential-algebraic equations (DAEs), sometimes called *implicit* or *singular* ODEs. Those concepts are based on the linear matrix pencils, their indices, and divergence of eigenvalues through infinity. After decades of developing such intriguing utilities, these instruments are not exhausted. So, we aim at concrete applications here (hoping to elucidate the versatility of tools from DAEs) and provide relevant pointers to the more abstract approaches. This paper links the SIB phenomenon [17,18] with the *transonic* flow in unsteady self-similar gravitational flows [21]. Two *implicit* ODE models from [6] are used to describe the SIB phenomenon and its properties in the self-similar transonic flow in gravitational fields around a central mass.

Basics: a regular dynamical system might be given by $\frac{dx}{dt} = f(x)$, $x \in \mathbb{R}^n$, while singular systems have the form $A(x) \cdot \frac{dx}{dt} = f(x)$ where the matrix A can be singular on its degeneracy/singularity set $\{x : \det A(x) = 0\}$. A prototypical degeneracy is that near the singular points, the speed $|\frac{dx}{dt}|$ can be infinitely large. This is evident from the simple-minded example $x \cdot \frac{dx}{dt} = 1$, $x \in \mathbb{R}$, which is singular at $x^* = 0$. The point x^* marks the sign-change of $\det A(x) = x$, which results in the velocity $\frac{dx}{dt}$ transitioning from

* Corresponding author.
E-mail address: tamdeber@tulane.edu (T. Amdeberhan).

https://doi.org/10.1016/j.physleta.2023.128896
0375-9601/

$+\infty$ to $-\infty$, when x switches from positive to negative values. In the higher-dimensional settings ($n > 1$), singular sets typically form co-dimension one surfaces in the phase space.

2. The scalar example

2.1. The isothermal case

Consider the isothermal case (meaning, the sound speed in the self-similar flow is spatially *constant*) described in [6] (see (10)-(12) in the Appendix)

$$g(s,V)\cdot\frac{dV}{ds}=f(s,V) \tag{1}$$

where in (12), the whole Newtonian approximation of the equations of motions and continuity is reduced to the nonlinear equation (1) in $V(s)$ only, with

$$\begin{aligned} g(s,V) &:= (V-\delta s)^2 - C^2 \\ f(s,V) &:= -\frac{1}{s}V(V-s)(V-\delta s) \\ &\quad + \frac{1}{s}(3V-\nu\delta s)C^2 - \frac{1}{s^2}(V-\delta s) \\ &\quad + \frac{1}{s}V\left[(V-\delta s)^2 - C^2\right]. \end{aligned}$$

The system (1) has singularity wherever $(V-\delta s)^2 - C^2 = 0$, which tantamount $M^2 = 1$, due to (11) (see the Appendix). Again, in the phase space, the curves (s,V) with $M^2 = 1$ form the *singular set* $\Sigma = \{g(s,V) = 0\}$ of the quasilinear DAE (1). The *equilibrium set* is $E = \{f(s,V) = 0, g(s,V) \neq 0\}$ and the *singular equilibrium set* is the intersection of Σ and the set of zeroes $\{f(s,V) = 0\}$ of f.

Analysis of (1) with (11) around $M = -1$ is discussed in this section. The case $M = 1$ can be analyzed in an analogous way.

Fig. 1 shows the solution trajectories of the above model obtained for $\nu = \mu = 0$ and $C = 1.2$. In order to cover the range of variables $-\infty < M \leq 0$, $0 \leq s < \infty$ the coordinates in Fig. 1 are transformed (see the labels of vertical and horizontal axes). The *sonic* points are those with $M = -1$ (horizontal line $M^2/(M^2+1) = 0.5$). All but three *sonic* points $S1$, N and $S2$ are the *impasse* points where trajectories either originate from or terminate at. The $S1$ and $S2$ are the sonic points where *folded saddles* are located, while the *sonic* point N is a *folded node*. Those concepts are explained in terms of the *algebraic* and *geometric* singularities of DAEs in [15,17] and illustrated in the context of traveling wave solutions of DAEs in [3,19]. The upper half of the square in Fig. 1 is the *supersonic* area with $-\infty < M < -1$, while the lower half is the *subsonic* area with $-1 < M < 0$.

Notice that one particular trajectory crosses the *sonic* line $M = -1$ three times. It originates in the upper left corner (*supersonic*) of the solution area, passes through $S1$ into the *subsonic* area, to reverse back into the *supersonic* area (through N), to move again into the *subsonic* area (through $S2$). There are two other *smooth subsonic-supersonic* trajectories crossing through $S1$ and $S2$. There exists also continuous (but not differentiable) trajectories crossing through N and either $S1$ or $S2$. They cover all possible transitions: *supersonic-subsonic-supersonic* and *subsonic-supersonic-subsonic*.

2.2. Singularity induced bifurcation in (1)

The above isothermal model with one differential and one algebraic equations (1) and (11), respectively, illustrates the SIB phenomenon present in some DAEs [3,17,19]. The *sonic* curve $M^2 - 1 = 0$ (or equivalently $(V-\delta s)^2 - C^2 = 0$) is the *singularity* of (1), which can be crossed by a smooth (at least C^1) trajectory if, in addition to $M^2 = 1$, the $f(s,V)$ in (1) is identically zero and its derivative with respect to s is non-zero at a sonic point. The SIB phenomenon in the context of the traveling wave solutions in two-phase fluid flow and similarity solutions in transonic inviscid flow in aerodynamics has been discussed in [3] and [15], respectively. The later item is particularly closely related to the topic of this paper, since both discuss the similarity solutions. Other areas where the SIB phenomenon was reported include the resistive MHD systems [19], electric power systems [18], and macroeconomics systems [9].

If $M = -1$, we have $h(s,V) := V - \delta s + C = 0$, which together with (1) form the dynamical system

$$g(s,V)\cdot\frac{dV}{ds} = f(s,V), \quad 0 = h(s,V), \tag{2}$$

yielding the matrix pencil

$$\{A,L\} := \left\{ \begin{pmatrix} \omega(s,V) & 0 \\ 0 & 0 \end{pmatrix}, \begin{pmatrix} df(s,V)/dV & df(s,V)/ds \\ 1 & -\delta \end{pmatrix} \right\} \tag{3}$$

with $\omega(s,V) := (V-\delta s)^2 - C^2$. This results in the characteristic equation

$$det(\lambda A - L) = \delta\omega(s,V)\lambda - \delta df(s,V)/dV - df(s,V)/ds = 0$$

and the eigenvalue

$$\lambda = \frac{n(s,V)}{\delta\omega(s,V)}$$
$$where \quad n(s,V) := \delta df(s,V)/dV + df(s,V)/ds. \tag{4}$$

Notice that $\omega(s,V)$ changes sign at each of the three *transonic* points $S1$, N and $S2$. When s increases, then $\omega(s,V)$ changes sign according to the pattern: $+/-$ at $S1$, $-/+$ at N and $+/-$ at $S2$. At the three sonic points $S1$, N and $S2$ the $n(s,V)$ is negative, positive and negative, respectively (see the values in the third and fourth columns in Table 1). Using this fact and the sign changes of $\omega(s,V)$ at the three *sonic* points, one can obtain the sign changes of λ as shown in the fifth column of Table 1; see also Fig. 2. The eigenvalue λ is negative on the left side (when $s < s_c$) and positive on the right side (when $s > s_c$) of each of the three *transonic* points.

The negative signs of λ as $s \to s_c^-$ and positive signs as $s \to s_c^+$ at each of the three points of interest indicate that the linear system is stable on the left side of each point (negative eigenvalue) and unstable on the right side (positive eigenvalue). Thus, the trajectory approaches each point of interest and moves away from that point after crossing the sonic line $M = -1$ in Fig. 1. Section 3.3 provides further discussion on the existence of smooth trajectories through the transonic points. Zeroing in on $\omega(s,V)$ at the three points (s_c, V_c) makes the values of λ diverge through infinity with $lim_{s\to s_c}\lambda = \pm\infty$. This is exactly the same behavior as in the SIB phenomenon in [17]. Moreover, the divergence of λ through infinity is equivalent to the increase of the *index* of the pencil (A,L) at $s = s_c$ [17]. The pencil (A,L) is of *index 0* when $s \neq s_c$ (because $det(A\lambda - L) \neq 0$) and *index 1* if $s = s_c$ ($det(A\lambda - L) = 0$). An example of the SIB phenomenon when the *index* increases from 1 to 3 at the bifurcation point (*singularity*) is discussed in [18] in the context of power systems DAEs.

One can also compute other properties of the smooth transonic solution at the points $S1$, N and $S2$ with variables used in Fig. 1(b), that is $W \equiv V/(|V| + s)$ and $z \equiv s/(s+1)$, and $M = -1$ (or $V_c = \delta s_c - C$), as follows

$$\begin{aligned} \frac{dW}{dz}_{|(s_c,V_c)} &= \left(\frac{dW}{dV}\frac{dV}{dz} + \frac{dW}{ds}\frac{ds}{dz}\right)_{|(s_c,V_c)} \\ &= \frac{(s_c+1)^2}{(|V_c|+s_c)^2}[(|V_c| + s_c - sign(V_c)V_c)\delta - V_c]. \end{aligned} \tag{5}$$

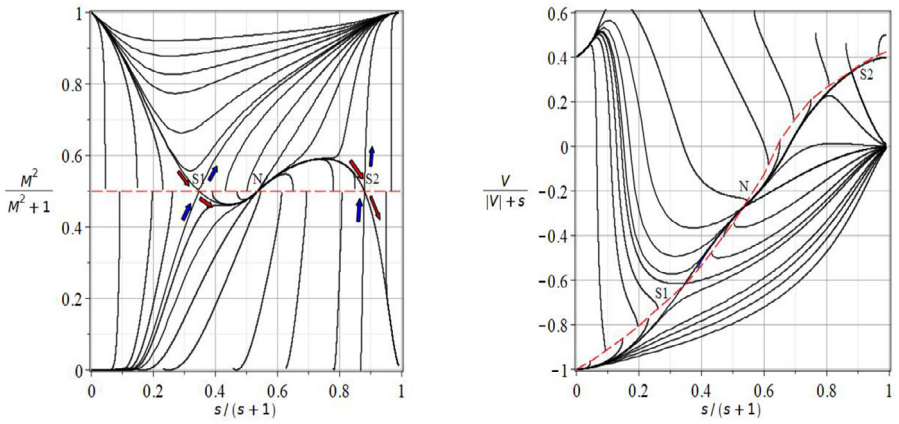

(a) Transonic crossings at $M=-1$. (b) As in Fig. 1(a) for variable V.

Fig. 1. Isothermal case: solution curves with crossings at the sonic points $S1$ and $S2$ (folded saddles) and N (folded node). The red dash line is the sonic curve $M=(V-\delta s)/C=-1$ for $\delta=2/3$ and $C=1.2$. A smooth trajectory crosses the sonic curve three times and is of the type: *supersonic* $(M<-1)\to$ *subsonic* $(-1<M<0)\to$ *supersonic* $(M<-1)\to$ *subsonic* $(-1<M<0)$ with $0<s<\infty$. The case $M<0$ is illustrated in both figures. There is a one-to-one correspondence between the respective trajectories in the two figures above.

Table 1
Data for $S1$, N and $S2$ for $\delta=2/3$.

point	(s_c, V_c)	$df(s_c,V_c)/dV$	$df(s_c,V_c)/ds$	$sign(\lambda)$	dW/dz (see (5))
$S1$	(0.5325, -0.8450)	1.2	-4.7753	$-\to+$	1.4852
N	(1.1559, -0.4294)	1.2	-0.0340	$-\to+$	2.2193
$S2$	(7.3117, 3.6745)	1.2	-1.0082	$-\to+$	0.6869

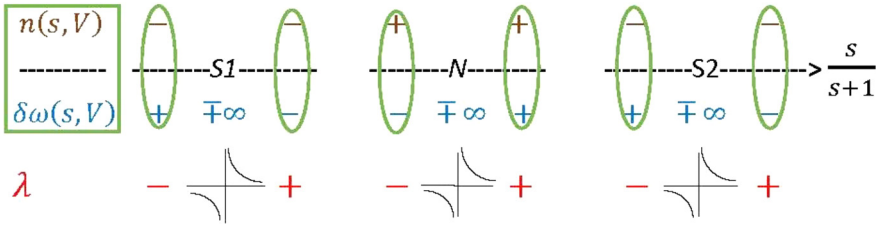

Fig. 2. The sign changes and divergence of λ through $\mp\infty$ at the $S1$, N and $S2$ transonic points.

The corresponding values of $\frac{dW}{dz}$ at the three transonic points are computed and shown in the last column of Table 1.

3. When $M=\pm1$ form two disjoint *sonic* (or Mach 1) curves

3.1. The (M,V) planar example

The Appendix provides the general model (12), which is equivalent to (10), and details about the self-similar variable s and the V and M dependent variables. Fig. 3 shows various trajectories of (12) for $\gamma=4/3$, $C=1.2$, $\delta=2/3$ and $\mu=\nu=0$. The values of horizontal variable $s/(s+1)$ close to 0 indicate either a small radius r for fixed time instant t, or large t for fixed value of r. For the horizontal variable $s/(s+1)$ being close to 1 we have large values of r with fixed t, or small t for fixed r. Notice the existence of one particular trajectory - the one passing through the two *folded saddles* with the direction marked by the red arrows in Fig. 3(a). The trajectory begins in the upper left corner in Fig. 3(a) for $s/(s+1)\approx0$ and ends in the lower right corner for $s\to\infty$, that is $s/(s+1)\to1$. The same trajectory is shown in Fig. 3(c) where the V and s variables are used. The trajectory is of the type *supersonic* $(M>1)\to$ *subsonic* $(|M|<1)\to$ *supersonic* $(M<-1)$ with two *transonic* crossings. There exist two other smooth *transonic* crossings (along the directions marked by the blue arrows in Figs. 3(a) and 3(c)). One of those trajectories passes through $M=1$ and the other through $M=-1$. The coordinates of the two *transonic* crossing points are: $M=1$ and $s=0.3333$ (equivalently, $M/(|M|+1)=0.5$, $s/(s+1)=0.25$) and $M=-1$, $s=1.631579$ (equivalently $M/(|M|+1)=-0.5$, $s/(s+1)=0.620000$).

3.2. Linearization for the (M,V) planar example around transonic points

If the right-hand sides of the two equations (12) are denoted by $f_1(s,M,V)$ and $f_2(s,M,V)$, respectively, then the linearization of that system around the two transonic points $M=\pm1$ (or $\mathcal{D}\equiv M^2-1=0$), can be analyzed through the linearized matrix

$$\mathcal{T}=\begin{pmatrix} \frac{\partial\mathcal{D}}{\partial s} & \frac{\partial\mathcal{D}}{\partial M} & \frac{\partial\mathcal{D}}{\partial V} \\ \frac{\partial f_1}{\partial s} & \frac{\partial f_1}{\partial M} & \frac{\partial f_1}{\partial V} \\ \frac{\partial f_2}{\partial s} & \frac{\partial f_2}{\partial M} & \frac{\partial f_2}{\partial V} \end{pmatrix}=\begin{pmatrix} 0 & \frac{\partial\mathcal{D}}{\partial M} & 0 \\ \frac{\partial f_1}{\partial s} & \frac{\partial f_1}{\partial M} & \frac{\partial f_1}{\partial V} \\ \frac{\partial f_2}{\partial s} & \frac{\partial f_2}{\partial M} & \frac{\partial f_2}{\partial V} \end{pmatrix} \tag{6}$$

whose singularity is due to the fact that $\frac{\partial f_1}{\partial s}\frac{\partial f_2}{\partial V}=\frac{\partial f_1}{\partial V}\frac{\partial f_2}{\partial s}$. The matrix $\mathcal{T}$ describes the dynamics of (12) in the following way: to determine the local behavior of (12) around the points with $M^2-1=0$ one needs to compute the two non-zero eigenvalues of $\mathcal{T}$, change the signs of those eigenvalues of $\mathcal{T}$ to opposite when $|M|<1$ (*subsonic* region) and keep the signs unchanged when $|M|>1$ (*supersonic* region) - see Section 3.3 for an explanation.

The three eigenvalues of T can be computed from (one of the eigenvalues is obviously zero)

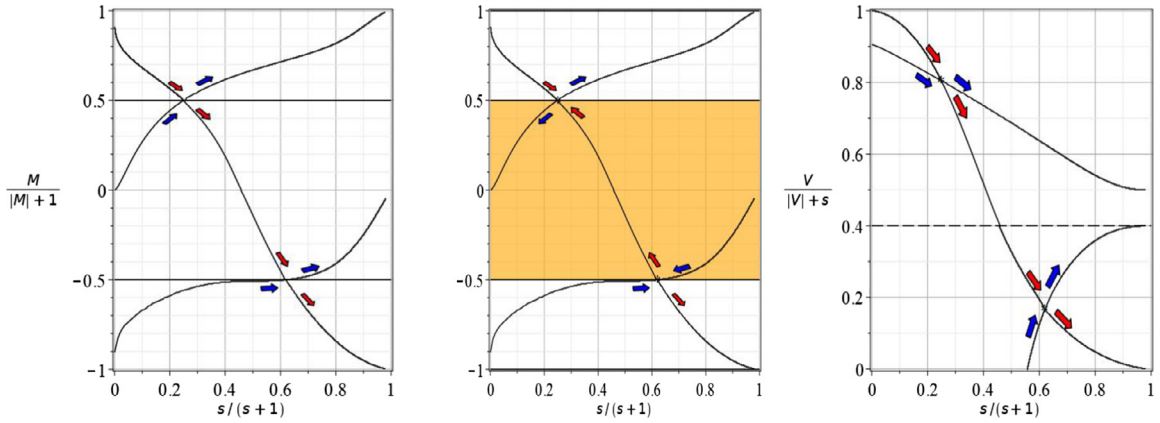

(a) Transonic crossings at $M=\pm 1$ for the system (12) having *folded saddles* at the transonic points with $M/(|M|+1)=\pm 0.5$.

(b) Shaded subsonic region and two *regular saddle* points for the *desingularized* system obtained from (12).

(c) As in Fig.3(a) for variable V.

Fig. 3. Trajectories of (12) for $\gamma=4/3$ and $\delta=2/3$ in Figs. (a) and (c) and *desingularized* model in Fig. (b). Shown are: (a) two transonic crossings *supersonic-subsonic-supersonic* with $M/(|M|+1)$ following the path $1\to 0.5\to -0.5\to -1$ while $s/(s+1))$ changes from 0 to 1 (the red-arrow path). Single transonic crossings occur along the blue-arrow paths. (b) saddle points for *desingularized* (12) with the shaded *subsonic* region $-0.5<M/(|M|+1)<0.5$ in which the flow is reversed compared to that in Fig. (a). The reversing is described and briefly justified in Section 3.3. (c) transonic-crossing path in variable V with two sonic points: the trajectory originates in the left upper corner for $s\approx 0$ (*supersonic* area) and ends in the right lower corner for $s/(s+1)\to 1$ and $V/(|V|+s)\to 0$ (*supersonic area* with $M<-1$). The middle part of that trajectory (between the two asterisks) is the *subsonic* range $|M|<1$. The transonic points ($M=\pm 1$) are marked with two asterisks and $M=0$ (or $V=\delta s$, see (11)) with the dash horizontal line. For $V=\delta s$ we have $V/(|V|+s)=\delta/(\delta+1)=const$, which equals 2/5 for $\delta=2/3$.

$$\lambda\left[\left(\lambda-\frac{\partial f_1}{\partial M}\right)\left(\lambda-\frac{\partial f_2}{\partial V}\right)-\frac{\partial f_1}{\partial V}\frac{\partial f_2}{\partial M}-2|M|\frac{\partial f_1}{\partial s}\right]=0 \tag{7}$$

where the $|M|$ term is to include both transonic points with $M=1$ and $M=-1$.

For the two transonic points shown in Fig. 3 we obtain

$$\begin{aligned}&\lambda(\lambda+19.277928)(\lambda-2.986459)=0\\ &\quad for\ M=1\ \ (s=0.333333,\ V=1.367917)\\ &\lambda(\lambda+4.463128)(\lambda-2.957500)=0\\ &\quad for\ M=-1\ (s=1.631579,\ V=0.325908)\end{aligned} \tag{8}$$

confirming the fact that $\mathcal{T}$ describes the *desingularized* system with real eigenvalues of opposite signs (resulting in two *regular saddle* points in Fig. 3(b)). This further yields, after changing the signs of eigenvalues for $|M|<1$, the *folded saddle* character of both transonic points for (12), see Fig. 3(a). Such a useful *desingularization* process of getting $\mathcal{T}$ for (12) and using it to obtain *folded saddles* in Fig. 3(a) from the *regular saddles* in Fig. 3(b), is described in more details, among others, in [15] and [17]. Further details of the solutions in Fig. 3 are provided in the figure caption.

3.3. Remarks on the sonic (singularity) crossing trajectory

The transonic (or singularity) crossing for (1) or (12) falls into the framework considered in [17] since, both of these models (equations) are *quasilinear* DAEs

$$A(s,x(s))x'=b(s,x(s)) \tag{9}$$

where $()'\equiv d/ds$. The *transonic* points are those *geometric* singularities $x^*:=x(s_c)$ of that DAE system with $b(s_c,x^*)\in\Im A(s_c,x^*)$, for which [17, Theorem 1] is applicable, leading to the conclusion of the existence of smooth C^1 *transonic* solutions. Here, $\Im A(s_c,x^*)$ denotes the image of $A(s_c,x^*)$. The local diffeomorphism used in [17, page 306] to obtain smooth *transonic* solution through x^* is the reason for the reversing of the s-direction when analyzing the solutions of (1) and (12) and their *desingularized* ODE models. For example, the diffeomorphism for the scalar case with singularity $\omega(s,V)$ (that is $dV/ds=f/\omega$ in (1), Section 2.1) is the integral $\xi(s)=\int_0^s\omega(\tau,y(\tau))d\tau$, where $y(s)$ is the solution of $y'=f(s,y)$, $y(0)=x^*$. When $\omega>0$ around x^* (*supersonic* region), then $\xi(s)$ is increasing and the integral curves of f are mapped into those of f/ω with the s-orientation (direction) being preserved. When $\omega<0$ near x^* (*subsonic* region), then $\xi(s)$ is decreasing, and the s-orientation (direction) is reversed along trajectories in that region. The two integral curves are used to obtain a C^1 trajectory satisfying $x(s_c)=x^*$. Such a reversal of the s-directions occurring in the subsonic region results in the reversals of the orbits of the *regular saddles* to yield the *folded saddles* for (9). See [17, page 307] for more details and [16] for a similar discussion on this topic.

Recall that *folded saddle point* P is a simple singular equilibrium of the DAE system for which the eigenvalues of the linearization matrix, say

$$\begin{pmatrix} f_x & f_y\\ g_xh & g_yh\end{pmatrix},$$

satisfy $\lambda_{1,2}\in\mathbb{R}$ and $\lambda_1\lambda_2<0$. It can be argued that the dynamics close to a folded saddle is determined by the eigenvectors associated to the eigenvalues of the corresponding (invariant) manifolds. The next result asserts that these eigenvectors are never tangent to Σ at (simple) singular equilibria.

Proposition. *If* $\mathbf{x_0}$ *is a folded saddle, then the eigenvectors (as directions) associated to eigenvalues* λ *are transverse to the singularity curve* Σ.

Proof. We proceed by contradiction. Suppose the eigenvector for some eigenvalue λ is tangent to Σ. Thus, the vector $(g_y,-g_x)^T$ tangent to Σ is an eigenvector of the linearized matrix:

$$\begin{pmatrix} f_x-\lambda & f_y\\ g_xh & g_yh-\lambda\end{pmatrix}\begin{pmatrix} g_x\\ -g_x\end{pmatrix}=\begin{pmatrix} f_xg_y-f_yg_x-\lambda g_y\\ g_x\lambda\end{pmatrix}=0$$

implying that either $g_x=0$ or $\lambda=0$, both conditions lead to a contradiction to the assumption that the singular equilibrium is simple. □

4. Conclusion

When self-similar flow crosses the *sonic* curve, the SIB phenomenon occurs. Such crossings from *supersonic* to *subsonic* regions (or the other way around) may happen multiple times by a single trajectory, as illustrated in this paper. When the SIB is not present at a *sonic* point, then that point is an *impasse* point, where the self-similar solution flow ceases to exist or where the flow originates from. One may argue that the *impasse* points are not physically acceptable, leading to the conclusion that the whole concept of transonic flows for mathematical models similar to (12), is flawed, and more complicated model is needed to incorporate physical phenomena without the possibility of the presence of *impasse* points. However, some other areas of science and engineering, for example the electric power system modeling, furnish examples of the system undergoing dramatic changes and losing stability - and researchers attempt to explain the collapsing electric power systems [22], by using the *singularity* crossing phenomena [13,18]. Also, the result in [10] is relevant with the discussion of self-similar Euler flows with gradient collapse (catastrophy) without shock formation.

CRediT authorship contribution statement

Wieslaw Marszalek: Conceptualization, Investigation, Validation, Writing – original draft. **Tewodros Amdeberhan:** Investigation, Methodology, Writing – original draft.

Declaration of competing interest

The authors declare that they have no known competing financial interests or personal relationships that could have appeared to influence the work reported in this paper.

Data availability

No data was used for the research described in the article.

Appendix A. The self-similar model: spherically symmetric gravitational field

Spherically symmetric unsteady flow in the gravitational field is described by a set of three equations (1)-(3) in [6] with the dependent variables v (velocity), p (pressure) and ρ (density), leading, through the adiabatic assumption and the self-similarity framework, to the following ODE model in the dependent variables (M, V) being functions of the independent similarity variable s, as follows

$$
\begin{aligned}
&(M^2-1)\frac{dM^2}{ds}\\
&=\frac{M^4}{s(V-\delta s)^2}\{2(\gamma-1)V^2+[-(3\gamma-1)\delta+\gamma-1]sV+2\delta s^2\\
&\quad+[4\gamma V+(\gamma+1)(2+\nu)\delta s-2s](V-\delta s)/(\gamma M^2)\\
&\quad-(\gamma+1)/s\}\\
&(M^2-1)\frac{dV}{ds}\\
&=\frac{1}{s(V-\delta s)}\{-V(V-s)M^2\\
&\quad+[3\gamma V+(2+\nu)\delta s-2s](V-\delta s)/\gamma\\
&\quad-M^2/s+V(V-\delta s)(M^2-1)\}
\end{aligned}
\tag{10}
$$

where $V(s)$ comes from the flow velocity $v=(Gm_0)^{1/3}t^{\delta-1}V(s)$, δ, ν and $C=s(\gamma P/D)^{1/2}=constant$ are some real constants, and $s=rt^{-\delta}/(Gm_0)^{1/3}$ is the similarity variable with G being the gravitational constant. Also, the m_0 is a constant in the time-dependent central mass expression $m=m_0t^{\mu}$, $\mu=3\delta-2$, γ is yet another constant, while $P(s)$ and $D(s)$ are the pressure and density similarity variables, and C is the sound speed. The $\gamma=4/3$ in Section 2 while it equals 1 in the simplified isothermal case considered in Section 3.

The instantaneous and local Mach number associated with the reference frame is defined as

$$M=(V-\delta s)/C \tag{11}$$

and the left-hand sides of (10) are equal zero if $(V-\delta s)^2-C^2=0$.

Using (11) we obtain $V-\delta s=CM$, so (10) can also be written as

$$
\begin{aligned}
&(M^2-1)\frac{dM^2}{ds}\\
&=\frac{M^2}{sC^2}\{2(\gamma-1)V^2\\
&\quad+[-(3\gamma-1)\delta+\gamma-1]sV+2\delta s^2-(\gamma+1)/s\}\\
&\quad+\frac{M}{s\gamma C}[4\gamma V+(\gamma+1)(2+\nu)\delta s-2s]\\
&(M^2-1)\frac{dV}{ds}\\
&=\frac{1}{sC}\{-V(V-s)M\\
&\quad+[3\gamma V+(2+\nu)\delta s-2s]C/\gamma-M/s+VC(M^2-1)\}
\end{aligned}
\tag{12}
$$

to form an equivalent system.

The most interesting case occurs when $M=1$ (or $M=-1$) and the right-hand sides in both equations in (12) are zero. Such cases are considered in this paper and lead to the *transonic* crossing trajectories with the derivatives of V and M being non-zero. Such crossings, sometimes called the *transonic* flows (or solutions) are considered in Sections 2 and 3 of this paper. Notice that due to the fact that $M=\pm1$, the *sonic* points form two separate (or disjoint) surfaces in the (s, M, V) space. See [4] for similar discussion.

References

[1] S. Anbar, S. Akin, Development of a linear predictive model for carbon dioxide sequestration in deep saline carbonate aquifers, Comput. Geosci. 37 (2011) 1802–1815, https://www.sciencedirect.com/science/article/pii/S0098300411001142.

[2] E.W. Beans, Shockless transition from supersonic to subsonic flow, J. Propuls. 11 (1994) 387–389, https://arc.aiaa.org/doi/abs/10.2514/3.51438.

[3] S.L. Campbell, W. Marszalek, DAEs arising from traveling wave solutions of PDEs, J. Comput. Appl. Math. 82 (1997) 41–58, https://www.sciencedirect.com/science/article/pii/S0377042797000848.

[4] A.F. Cheng, Time-dependent fluid flow in a central gravitational field, Astrophys. J. 213 (1977) 537–547, https://www.osti.gov/biblio/7313267.

[5] C. Courtois, C. Robert, D. Bretheau, J. Fariaut, M. Ferri, I. Geoffray, G. Legay, F. Phillipe, R. Roche, G. Soullie, B. Villette, Supersonic-to-subsonic transition of a radiation wave observed at the lmj, Phys. Plasmas 28 (2021) 073301, https://aip.scitation.org/doi/10.1063/5.0054288.

[6] J. Fukue, Self-similar transonic flow in the spherically symmetric gravitational field, Publ. Astron. Soc. Jpn. 36 (1984) 87–103.

[7] K.G. Guderley, The Theory of Transonic Flow, Pergamon Press, Oxford, 1962.

[8] S. He, Z. Yang, Y. Gu, Nonlinear dynamics of an aeroelastic airfoil with free-play in transonic flow, Nonlinear Dyn. 87 (2017) 2099–2125, https://doi.org/10.1007/s11071-016-3176-4.

[9] Y. He, W.A. Barnett, Singularity bifurcations, J. Macroecon. 28 (2006) 5–22, https://www.sciencedirect.com/science/article/pii/S0164070405000704.

[10] H.K. Jenssen, A.A. Johnson, New self-similar euler flows: gradient catastrophe without shock formations, https://arxiv.org/abs/2205.15876, 2022. (Accessed 15 March 2023).

[11] A.M. Kuethe, C.Y. Chow, Foundations of Aerodynamics: Bases of Aerodynamic Design, 5th ed., New York, Wiley, 1997.
[12] P. Künzli, K. Tsunematsu, P. Albuquerque, J.L. Falcone, B. Chopard, C. Bonadonna, Parallel simulation of particle transport in an advection field applied to volcanic explosive eruptions, Comput. Geosci. 89 (2016) 174–185, https://www.sciencedirect.com/science/article/pii/S0098300416300309.
[13] H. Kwatny, A. Pasrija, L. Bahar, Static bifurcations in electric power networks: loss of steady-state stability and voltage collapse, IEEE Trans. Circuits Syst. 33 (1986) 981–991, https://ieeexplore.ieee.org/document/1085856.
[14] Mach1Airspace, Blue angel in high speed mach pass w/ vapor wave, https://www.youtube.com/watch?v=e8kUf8HSu3k, 2015. (Accessed 15 March 2023).
[15] W. Marszalek, Fold points and singularity induced bifurcation in inviscid transonic flow, Phys. Lett. A 376 (2012) 2032–2037, https://www.sciencedirect.com/science/article/pii/S0375960112005488.
[16] W. Marszalek, A DAE approach to similarity solutions of unsteady fluid flows: an application case study, in: 2014 American Control Conference, 2014, pp. 5145–5149, https://ieeexplore.ieee.org/document/6858785.
[17] W. Marszalek, T. Amdeberhan, R. Riaza, Singularity crossing phenomena in daes: a two-phase fluid flow application case study, Comput. Math. Appl. 49 (2005) 303–319, https://www.sciencedirect.com/science/article/pii/S0898122105000350.
[18] W. Marszalek, Z.W. Trzaska, Singularity-induced bifurcations in electrical power systems, IEEE Trans. Power Syst. 20 (2005) 312–320, https://ieeexplore.ieee.org/document/1388524.
[19] W. Marszalek, Z.W. Trzaska, New solutions of resistive mhd systems with singularity induced bifurcations, IEEE Trans. Plasma Sci. 35 (2007) 509–515, https://ieeexplore.ieee.org/document/4154883.
[20] J.G. Park, W.S. Han, G. Han, J. Piao, S. Kwon, Characterization of choked conditions under subsonic to supersonic flow in single-phase (supercritical to gaseous CO_2 or liquid H_2O) and multiphase (CO_2 and H_2O) transport, J. Geophys. Res., Solid Earth 124 (2019) 3570–3587, https://agupubs.onlinelibrary.wiley.com/doi/10.1029/2018JB016824.
[21] S. Sakashita, M. Yokosawa, Similarity solution for unsteady accretion flow ii, Astrophys. Space Sci. 31 (1974) 251–259, https://link.springer.com/article/10.1007/BF00642615.
[22] B. Schäfer, D. Witthaut, M. Timme, V. Latora, Dynamically induced cascading failures in power grids, Nat. Commun. 9 (2018), https://doi.org/10.1038/s41467-018-04287-5.
[23] P. Weinacht, A Direct-Fire Trajectory Model for Supersonic, Transonic, and Subsonic Projectile Flight, Army Research Laboratory, 2014, https://apps.dtic.mil/sti/pdfs/ADA607593.pdf.
[24] W. Zhang, C. Gao, Y. Liu, Z. Ye, Y. Jiang, The interaction between flutter and buffet in transonic flow, Nonlinear Dyn. 82 (2015) 1851–1865, https://link.springer.com/article/10.1007/s11071-015-2282-z.